Isı Bilimi ve Tekniği Dergisi, 35, 2, 53-62, 2015
J. of Thermal Science and Technology

ISSN 1300-3615

SIZING OF A TURBOPROP UNMANNED AIR VEHICLE AND ITS PROPULSION SYSTEM

Ali DİNÇ
Tusaş Engine Industries Inc., Çevreyolu No: 356, 26003 Eskişehir, Turkey, alidinc@yahoo.com

(Geliş Tarihi: 29.05.2014, Kabul Tarihi: 01.03.2015)

Abstract: In this study, a genuine computer code for sizing of an unmanned aerial vehicle (UAV) and its turboprop engine by analytical method is developed. Payload and fuel weights are primary factors affecting UAV size and weight (which need to be fulfilled in terms of flight performance parameters, e.g. lift and drag). The parameters within mission profile such as altitude, speed of aircraft are keys for selecting engine type. Engine specific fuel consumption (SFC) defines the total fuel amount to be stored and carried during the flight, which affects the general dimensions and the gross weight of the aircraft. Some engine parameters namely, compressor pressure ratio and turbine inlet temperature, have direct influence on SFC. Turboprop engine subroutine code developed in this study is within ±1% agreement with commercial engine cycle analysis software "GasTurb" for shaft power, propeller thrust and SFC etc. values, at all mission points of UAV. Calculated weight, size, endurance values of UAV are seen to be close to literature values. Literature values indicate some inconsistencies especially for endurance and empty weight of aircraft. Considering most dependable references and logical combinations of inputs, error in calculation of UAV weight and size is about ±1,5% and for maximum operating altitude is around ±3%. Moreover, calculated endurance values are within range of literature values.
Keywords: unmanned air vehicle design, aircraft sizing, propulsion, turboprop, gas turbine engine, cycle analysis

BİR TURBOPROP İNSANSIZ HAVA ARACININ VE İTKİ SİSTEMİNİN BOYUTLANDIRILMASI

Özet: Bu çalışmada, bir insansız hava aracının (İHA) ve turboprop motorunun analitik yöntemle boyutlandırılması için özgün bir bilgisayar yazılımı geliştirilmiştir. Faydalı yük ve yakıt ağırlıkları, İHA boyut ve ağırlığını (taşıma ve sürükleme kuvvetleri gibi temel uçuş performans parametreleri açısından karşılanması gereken) etkileyen başlıca faktörlerdir. Görev profilindeki irtifa, uçak hızı gibi parametreler, motor tipini seçmek için anahtardır. Motor özgül yakıt tüketimi (SFC) uçağın genel boyutlarını ve toplam ağırlığını etkileyen ve uçuş sırasında depolanıp taşınacak olan toplam yakıt miktarını tanımlar. Kompresör basınç oranı ve türbin giriş sıcaklığı gibi bazı motor parametrelerinin, SFC üzerinde doğrudan etkisi vardır. Bu çalışma kapsamında geliştirilen turboprop motor alt yazılımı İHA'nın tüm görev noktalarında mil gücü, pervane itkisi, SFC vb. değerler için ticari motor çevrim analiz yazılımı olan "GasTurb" ile ±%1 uyum içerisindedir. İHA'nın hesaplanan ağırlık, boyut, dayanıklılık değerlerinin literatür değerlerine yakın olduğu görülmüştür. Literatür değerleri, özellikle azami uçuş süresi (endurance) ve uçak boş ağırlığı için tutarsızlıklar göstermektedir. En güvenilir referanslar ve girdilerin mantıksal kombinasyonları göz önüne alındığında, İHA ağırlığı ile boyutundaki hesaplama hatası yaklaşık ±%1,5 ve azami uçuş irtifası ±%3 olarak hesaplanmıştır. Ayrıca, hesaplanan azami uçuş süresi değerleri literatürde verilen aralıklardadır.
Anahtar Kelimeler: insansız hava aracı tasarımı, uçak boyutlandırma, itki, turboprop, gaz türbin motoru, çevrim analizi

NOMENCLATURE

a_i	speed of sound at engine station "*i*" [m/s]
A_7	exhaust nozzle area [m^2]
$A_{7,c}$	nozzle exit area for choking condition [m^2]
AIAA	American Institute of Aeronautics and Astronautics
AR	aspect ratio of wing [dimensionless]
c	chord length [m]
C	specific fuel consumption [kg/(kN.h)]
C_{corr}	engine airflow correction factor [dimensionless]
C_F	thrust coefficient of propeller [dimensionless]
C_{fe}	surface friction coefficient [dimensionless]
C_{ff}	composite fudge factor for fuselage [dimensionless]
C_{fht}	composite fudge factor for horizontal tail [dimensionless]
C_{fvt}	composite fudge factor for vertical tail [dimensionless]
C_{fw}	composite fudge factor for wing [dimensionless]
C_L	lift coefficient [dimensionless]
C_{Lmax}	maximum lift coefficient [dimensionless]
$C_{L,\ TO}$	max. lift coefficient for take of [dimensionless]
C_{PC}	specific heat for compressor [kJ/kg K]
C_{PT}	specific heat for turbine [kJ/kg K]
C_{PW}	power coefficient of propeller [dimensionless]
d	propeller diameter [m]
d_{cl}	climb distance (in horizontal) [km]
D	drag force [N]

e	Oswald efficiency for wing [dimensionless]
E	Endurance [h]
EPW	Equivalent shaft power [kW]
ESFC	Equivalent power specific fuel consumption [kg/(kW.h)]
f	fuel air ratio [kg/kg]
$f_{fus.vol}$	fuselage volume utilization factor [m^3/m^3]
$f_{fus.vol.m}$	fuselage volume margin [m^3/m^3]
f_{lg}	landing gear weight ratio [kg/kg]
f_{misc}	other misc. equipment weight ratio [kg/kg]
$f_{nac.wet}$	nacelle wet area factor [m^2/m^2]
F_{net}	net total thrust [N]
$f_{resfuel}$	landing reserve fuel ratio [kg/kg]
f_{sys}	avionics and flight systems weight ratio [kg/kg]
$f_{th.ins}$	thrust installation loss factor [N/N]
$f_{w.eng}$	engine installation weight factor [kg/kg]
f_{wm}	empty weight margin [kg/kg]
F_A	nozzle thrust [N]
G_C	Power required for compressor [kW]
G_{HPT}	power generated by high pressure turbine [kW]
G_{LPT}	power generated by low pressure turbine [kW]
h	aircraft flight altitude [km]
h_0	altitude for takeoff (point 1) [km]
h_{10}	altitude for landing (point 10) [km]
h_{34}	altitude at the end of climb or at the start of cruise (points 3−4) [km]
h_{56}	altitude at the end of cruise or at the start of loiter (points 5−6) [km]
h_{78}	altitude at the end of loiter or at the start of cruise (points 7−8) [km]
h_9	altitude at the end of return cruise or at the start of descent (point 9) [km]
J	advance ratio [dimensionless]
L	lift [N]
L/D	lift to drag ratio [N/N]
L_{fus}	total fuselage length [m]
$L_{fus.b}$	fuselage back side cone length [m]
L_{nac}	nacelle length [m]
M_0	flight Mach number [dimensionless]
n	propeller speed [rev/s]
n_{eng}	number of engines
n_{fus}	number of fuselage of aircraft
N_{cd}	nozzle discharge coefficient
N_{cx}	nozzle thrust coefficient
P_i	total pressure at station "*i*" [kPa]
P_{amb}	ambient static pressure [kPa]
PLA_{idle}	engine idle throttle percent [%]
PSFC	power specific fuel consumption [kg/(kW.h)]
PW	uninstalled engine shaft power [kW]
R	range [km]
RASCE	Rapid Air System Concept Exploration tool
R_{CL}	climb distance [km]
R_{CR}	cruise range [km]
R_D	descent distance [km]
R_F	range [km]
R_{op}	operation radius of UAV [km]
S	total wing area [m^2]
S_h	horizontal tail area [m^2]
S_v	vertical tail area [m^2]
t/c	thickness to chord ratio of wing [m/m]
t_{ave}	average thickness of wing airfoil [m]
t_{max}	maximum thickness of wing airfoil [m]
t_B	block time [h]
t_{CL}	climb time [h]
t_{CR}	cruise time [h]
t_D	descent time [h]
t_F	flight time [h]
t_{GR}	ground maneuver time [h]
t_{idle}	idle time before takeoff [h]
T_{inst}	installed thrust (propeller+jet)
t_{loi}	loiter time [h]
t_{pow}	time of maximum power for take-off [min]
t_{tot}	total mission time [h]
t_{wait}	maximum waiting time spent on air before landing [min]
T_{amb}	ambient static temperature [K]
T_{bleed}	Compressor middle stage total temperature for bleed [K]
T_i	total temperature at station "*i*" [K]
TSFC	thrust specific fuel consumption [gr/(kN.s)]
T_{uninst}	uninstalled thrust (propeller+jet) [N]
u_{fus}	unit weight for aircraft fuselage and nacelle [kg/m^2]
u_{htail}	unit weight for the horizontal tail [kg/m^2]
u_{vtail}	unit weight for the vertical tail [kg/m^2]
u_{wing}	unit weight for wings [kg/m^2]
UAS	unmanned air system
UAV	unmanned air vehicle
V_0	aircraft flight velocity [km/h]
V_{climb}	climb speed [km/h]
V_{stall}	stall speed [km/h]
V_{cr}	maximum cruise speed [km/h]
V_{fuel}	fuel volume [m^3]
V_{wing}	wing volume [m^3]
V_{loi}	max. speed (Mach number) for loiter and climb
V_{stall}	stall speed [km/h]
V_{ref}	reference speed for takeoff [km/h]
V_{wind}	headwind [km/h]
w_i	engine airflow at station "*i*" [kg/s]
w_f	fuel flow [kg/s]
W/S	wing loading [kg/m^2]
W	aircraft weight during flight stages [kg]
W_0	maximum aircraft gross weight [kg]
W_{af}	airframe weight [kg]
W_e	aircraft empty weight [kg]
W_{eng}	engine weight [kg]
W_f	total fuel weight [kg]
W_{fe}	external fuel weight [kg]
W_{fi}	internal fuel weight [kg]
W_{fus}	fuselage weight [kg]
$W_{h.tail}$	horizontal tail weight [kg]
W_{lg}	landing gear weight [kg]
W_{misc}	miscellaneous weight [kg]
W_{nac}	nacelle weight [kg]
W_{Pe}	external payload weight [kg]
W_{Pi}	internal payload weight [kg]
W_{PL}	total payload weight [kg]
W_{sys}	systems weight [kg]
$W_{v.tail}$	vertical tail weight [kg]

Greek Symbols

ΔP_b	total pressure loss in combustion chamber [kPa/kPa]

ΔP_{in}	intake total pressure loss [dimensionless]
$\Delta P_{j.pipe}$	total pressure loss of the low pressure turbine jet pipe [dimensionless]
$\Delta P_{t.duct}$	total pressure loss in the duct between high and low pressure turbines [kPa/kPa]
$Ø_{eng}$	engine diameter [m]
$Ø_{fus}$	fuselage diameter [m]
$Ø_{nac}$	nacelle diameter [m]
$Ø_{nac}$	nacelle diameter [m]
$Ø_{prop}$	propeller diameter [m]
β_1	compressor middle stage bleed air ratio [dimensionless]
γ	specific heat ratio [dimensionless]
δ	atmospheric pressure ratio [$=P_{amb}/P_{SL}$]
ε_1	compressor middle stage air extraction ratio for low pressure (LPT) duct cooling
ε_{2a}	cooling air ratio for high pressure turbine
ε_{2b}	cooling air ratio for low pressure turbine duct
ε_3	cooling air ratio nozzle guide vanes (NGV)
η_2	compressor isentropic efficiency
η_{416}	high pressure turbine isentropic efficiency
η_{46}	low pressure turbine isentropic efficiency
η_b	combustor efficiency
$\eta_{C,pol}$	compressor polytrophic efficiency
η_m	mechanical efficiency
η_p	propeller efficiency (constant or function of J)
$\eta_{prop,d}$	propeller dynamic efficiency
$\eta_{prop,s}$	propeller static efficiency
$\eta_{T,pol}$	turbine polytrophic efficiency
θ	atmospheric temperature ratio [$=T_{amb}/T_{SL}$]
λ	tip to hub chord length ratio of wing
Π_C	compressor total pressure ratio
Π_N	exhaust nozzle pressure ratio (design input)
Π_T	turbine total pressure ratio
ρ_{eng}	uninstalled engine density
ρ_{fuel}	fuel density
ρ_{lg}	landing gear density
ρ_{pl}	payload density
ρ_{sys}	systems density
Ω_{prop}	propeller speed [rpm]

INTRODUCTION

It has been more than a century since Wright brothers realized the first controlled, powered and sustained heavier-than-air human flight in 1903. Aviation industry is one of the emerging high-tech fields, starting from the period of First World War and studies in this field indicate that importance of the aviation sector will increase in the coming years (Genç et al., 2008). Many types of aircraft with different complexity have been designed and built over the past century as the technology advanced.

In addition to manned aerial vehicles, unmanned or uninhabited air vehicles (UAV) have been developed as well. As defined in the AIAA Committee of Standards', "Lexicon of UAV, ROA (remotely operated aircraft) Terminology, a UAV is "an aircraft which is designed or modified, not to carry a human pilot and is operated through electronic input initiated by the flight controller or by an onboard autonomous flight management control system that does not require flight controller intervention". The suitability of UAVs in "dull, dirty and dangerous" missions, the increasing success of UAVs in service and demonstration. Therefore, UAV is an aircraft which can autonomously fly or can be remotely controlled to perform a specific mission without flying crew inside. Unmanned air vehicles have a lot of varieties including micro, tactical, strategic and combat types (Chaput, 2004).

An over-simplistic view of an unmanned aircraft is that it is an aircraft with its aircrew removed and replaced by a computer system and a radio-link. In reality it is more complex than that, and the aircraft must be properly designed, from the beginning, without aircrew and their accommodation, etc. (Austin, 2010).

Design of a UAV is similar to that of a manned aircraft to some extent. A lot of tools and methods were developed in the past for aircraft design. Some of the well-known text books published in literature belong to Raymer (1999), Roskam (1990) and Nicolai (2010). Sizing codes were generated to speed up the conceptual design phase using the developed aircraft design methodology. Some are simple in-house parametric sizing codes and some are sophisticated commercial programs (Internet, 2014). Parametric codes are typically used for concept exploration. One example is Rapid Air System Concept Exploration (RASCE) tool which is a physics-based, unmanned air system conceptual level design and analysis system. RASCE is originally developed as an educational tool to support undergraduate student exploration (Chaput, 2010).

For aircraft design, mission profile definition consists of a very important set of parameters. A mission profile is a scenario that is required to establish the weight, fuel, payload, range, speed, flight altitude, loiter and any other operations that the aircraft must be able to accomplish. The mission requirements are specific to the type of the aircraft (Curtis et al., 2009). In other words, mission profile is a scheme of aircraft's flight segments and detailed description of aircraft activities in flight. For this reason, it is very important for the design of the aircraft. Figure 1a, shows a typical reconnaissance unmanned air vehicle mission profile. A representative mission profile is assumed for this study and shown in Figure 1b. A total of 11 mission points are defined from start to end. Descriptions of all those 11 points are given in Table 1.

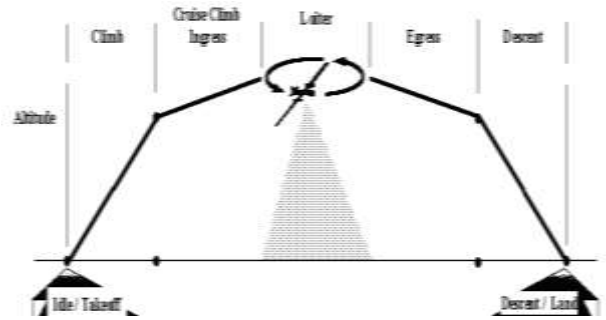

Figure 1a. A typical reconnaissance unmanned air vehicle mission profile (Federation of American Scientists, 2014).

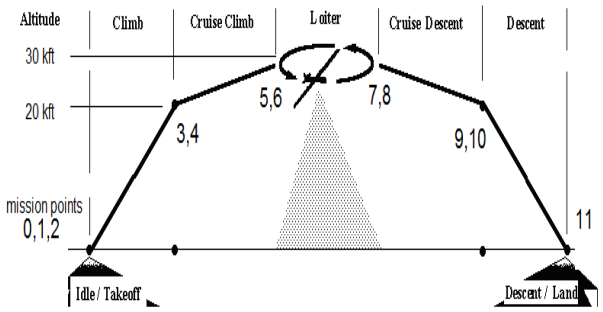

Figure 1b. A representative mission profile for Predator B.

Table 1. Predator B assumed mission profile.

Mission Point	Description	Mission Altitude
0	Idle	0
1	Taxi and take off	0
2	End of take-off, start of climb	0
3	End of climb	6,096 km (20 kft)
4	Start of cruise climb	6,096 km (20 kft)
5	End of cruise climb	9,144 km (30 kft)
6	Start of loiter	9,144 km (30 kft)
7	End of loiter	9,144 km (30 kft)
8	Start of cruise descent	9,144 km (30 kft)
9	End of cruise descent	6,096 km (20 kft)
10	Start descent	6,096 km (20 kft)
11	Landing	0

SIZING OF UNMANNED AIR VEHICLE

For the sizing of UAV, general aircraft weight formulae can be used by omitting crew and passenger weights (Raymer, 1999). In Figures 2a-2b, a simplified geometry is created genuinely for this study by inspiration from real UAVs such as "Predator B". The UAV in Figures 2a-2b consists of basic cylinder, sphere, cone etc. shapes which make calculations (e.g. volume, area) simpler. The volume and area values for UAV components (wing, fuselage etc.) are used for weight estimation. Related component weight formulae and densities are taken from Chaput (2004) and Raymer (1999).

Figure 2a. A simplified geometry UAV, 3-dimensional view.

Figure 2b. A simplified geometry UAV, side view.

AIRCRAFT PERFORMANCE

Although intensive test data and accumulated experience are needed for accurate estimates of performance in the later stages of design, the equations used in this study will be simple, basic and are sufficient for the preliminary design stage. Flight durations and range calculations (Buğdaycı, 1980) are given in equations section.

PROPULSION

Different propulsion systems are used to power aircraft to fly. Piston, electric, gas turbine, ramjet, scramjet and even nuclear engines are used in commercial and military aviation. Turbofan, turbojet, turboshaft and turboprop engines are in the group of gas turbine engines. Gas turbine engines, based on terrestrial and aeronautical, are used for a wide range of power generation applications, including aerospace, cogeneration, power plants and the like (İlbaş and Türkmen, 2012).

The general energy supply and environmental situation requires an improved utilization of energy sources. Therefore, the complexity of power-generating units has increased considerably. This requires thermodynamic calculations of high accuracy (Şahin et al., 2011).

As explained by Chaput (2010), satisfying propulsion data requirements can be a problem, particularly for students. Air vehicle performance codes typically require tabular inputs of installed thrust and fuel flow. Generating the installed data can be time consuming and/or involve use of proprietary engine company codes. One solution to the problem is to use an integrated multi-discipline parametric design system that has the fidelity of a conceptual point design and analysis system and the flexibility of a parametric sizing code.

Structuring an aero-thermal model of a gas turbine engine is the first step to simulate engine performance in a dynamic manner (Uzol, 2011). The object of parametric cycle analysis is to obtain estimates of the performance parameters (power/thrust and specific fuel consumption) in terms of design limitations (such as maximum allowable turbine temperature and attainable component efficiencies), the flight conditions (the ambient pressure, temperature and Mach number) and design choices (e.g. compressor pressure ratio) (Mattingly et al., 2002). Parametric analysis determines the engine performance under different flight conditions, different design choices (e.g. compressor pressure ratio) and design constraints (e.g. burner exit temperature); whereas the performance analysis allows the calculation of performance for different flight conditions and power level of the engine with determined specific values (Turan et al., 2008).

"Predator-B" UAV uses TPE331−10 turboprop engine (Honeywell, 2014). Therefore in this section, a detailed turboprop engine on-design cycle analysis is studied, although in RASCE tool developed by Chaput (2010), turboprop performance is simply modeled as a turbofan of very high bypass ratio.

In Figure 3, schematic of a two spool turboprop engine is shown. Main components are intake (A), compressor (B), burner (C), high pressure turbine (D), low pressure turbine (E) and finally exhaust nozzle (F). Methodology in Walsh and Fletcher (2004) is used for turboprop cycle analysis in general, with the exception that similar to method in Kurzke (2007), burner exit temperature is taken as design parameter instead of stator outlet temperature.

A two spool turboprop engine design point calculations are given in Equations section.

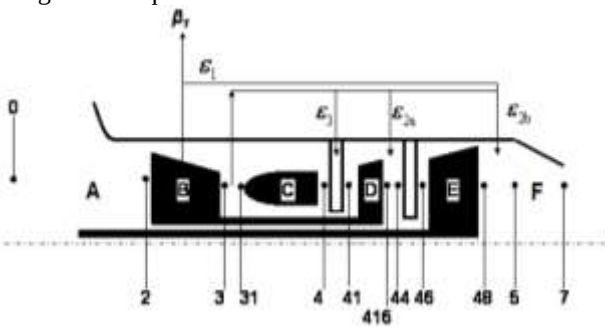

Figure 3. Schematic view of two spool turboprop engine (Walsh and Fletcher, 2004).

A CODE FOR SIZING UAV AND ITS ENGINE

Putting together all information (aircraft and engine sizing, performance equations), a genuine code for sizing a turboprop UAV is written for both aircraft and its engine. Some empirical data and correlations are also used for some parameters such as weight estimation of engine, UAV components and systems. The code is about 1000 lines including engine subroutine.

In Figure 4, flowchart of UAV and Turboprop engine sizing code is given. Code starts with an initial size for aircraft and engine, but updates (decrease or increase) the size of both aircraft and engine through iterations for the given inputs. At the end it converges to a final size, weight, performance of engine and UAV.

More than 100 parameters (related with mission profile aircraft and engine design options/selection/limits etc.) are used in the input file (see Table 3).

Conf. 1 input values are given in Table 3. There are 3 configurations of UAV as follows:

- Conf.1: With external fuel tanks and 1/3 of weapons
- Conf.2: Clean configuration (no external fuel tanks or weapons)
- Conf.3: With full weapons (no external fuel tanks)

In Table 3, input data and configuration information are collected from literature (Chaput, 2004; Raymer, 1999; Honeywell, 2014; General Atomics Aeronautical Systems, 2014; Defense Technical Information Center, 2003; Executive Aircraft Maintenance, 2014) and sub grouped into mission, aircraft weight, aircraft aero, aircraft components and finally engine specific segments. Some data are not available in literature and are best guessed to match the overall performance parameters. For example, engine parameters like $\eta_{C,pol}$, $\eta_{T,pol}$, η_b , η_m , ε_1 , ε_{2a} , ε_{2b} , ε_3 etc. are best guesses to match the power and SFC values.

For a different run, if any of the inputs in Table 3 is changed, then both aircraft and engine size and performance parameters change. For example, if payload is changed as an input, aircraft size changes to carry this additional weight by increasing the wing area (for the given wing loading). Then engine size change as a result for new size aircraft needs, after iterations. Similarly, if fuel weight is changed as an input, aircraft size changes for fuel storage and similarly engine size and performance (endurance, range etc.) change as well, again after automatic iterations.

There are some checkpoints in the code and gives warning messages if any of the following illogical cases occur. Then inputs should be reviewed:

- Too low thrust to balance drag, for the input altitudes (decrease altitude or increase engine power)
- Too low input velocity to produce required lift (increase cruise or loiter Mach number)
- Complex numbers in results (check engine and aircraft parameters)
- Negative numbers in flight time segments, climb rate etc. (check engine and aircraft parameters)

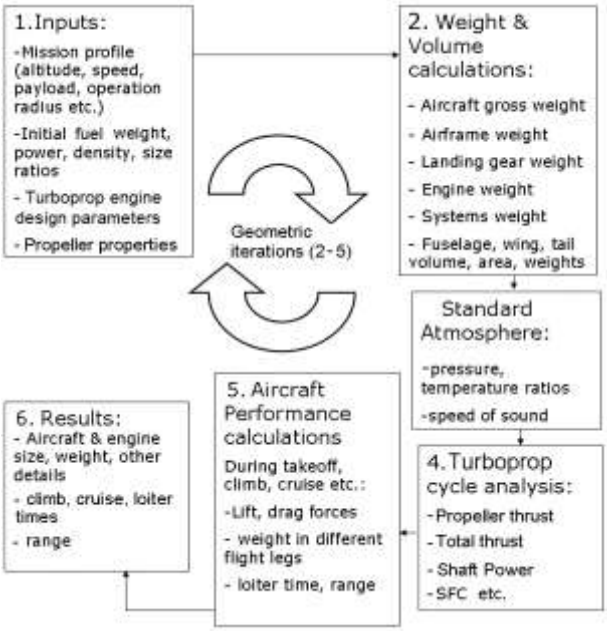

Figure 4. Flowchart of UAV and turboprop engine sizing code.

RESULTS AND DISCUSSION

For an assumed Predator-B configuration (per inputs in Table 3), code is run and results are given in Table 2 and 4. Literature and calculated values are compared and are found to be close. Literature values are somehow inconsistent especially for the endurance, empty weight, internal fuel storage amount which does not make clear targets for the computer model or code to match, mainly due to official detail data is limited and there are a lot of

versions developed in time for the Predator B and also external payload and fuel amount may vary in configurations of UAV. However most dependable references and logical combinations are checked and presented. In Table 2, only overall parameters are given as a summary and comparison is made with literature values. Mathematical model is robust and for 3 different configurations calculated error for UAV weight and size is about ±1,5%, maximum operating altitude is around ±3% and endurance is within given literature intervals.

In Table 4, selected resulting parameters are listed after calculations. Aircraft sizing (e.g. weight, wing area) and performance (endurance, range, drag etc.) parameters are calculated. In addition, engine related parameters such as power, SFC and all pressure and temperature values at different stations are given. Those aircraft and engine related parameters are close to benchmark model Predator B and its engine TPE331−10.

Table 2. Predator-B data comparison (General Atomics Aeronautical Systems, 2014; UK Royal Air Force, 2014; Defense Technical Information Center, 2003; Department of the Air Force Headquarters Air Force Civil Engineer Support Agency, 2009; Department of Defense, 2009).

Parameter	Literature Value	Calculated value	Error %
Max Gross Takeoff Weight	4763 kg (Conf. 1-3) 3454 kg (Conf. 2)	4770 kg 3403 kg	0,15% 1,5%
Empty Weight	1863- 2227 kg (Conf. 1-2-3)	2184 kg	in range
Dimension: Wingspan Length Fuselage diameter	20,11 m 10,97 m 0,91−1,13 m (Conf. 1-2-3)	20,13 m 10,97 m 1,02 m	0,1%
Max Operating Altitude	15,24 km (Conf. 2)	14,78 km	3,1%
Maximum Endurance (hours)	27-32 (Conf. 1) 20-24 (Conf. 2) 12-14 (Conf. 3)	31,28 22,26 12,96	in range
Engine Parameter: EPW ESFC	704 kW 0,325 kg/kW/h (Conf. 1-2-3)	702,2 kW 0,3258 kg/kW/h	0,25%

Additionally, calculated engine parameters by code are compared with a commercial engine cycle analysis software GasTurb (Kurzke, 2007) and maximum differences are given in Table 5. For each mission point (see Table 1), code makes the on-design calculations and results are within ±1% agreement with GasTurb as can be seen in Table 5.

CONCLUSION

As the unmanned air vehicles become more common and useful systems in both military and civil area, fast and efficient design tools are needed in every stage of development process. The genuine computer code developed in this study can be used in the preliminary stage of design for initial sizing of aircraft. Input parameters are calibrated and the results obtained are close to benchmark model values (Predator B). This kind of fast tools can be beneficial especially in the conceptual design iterations before going into detailed design. The code has a detailed engine cycle analysis subroutine and can be used both aircraft designers and engine designers. Aircraft designers can use this detailed engine subroutine for propulsion calculations (when they need a so-called rubber engine) and engine designers can use it to start a new engine design by seeing direct effects of engine design parameters on aircraft sizing and performance. Similarly students can use this kind of educational tool to see the effect of an engine or aircraft parameter on the overall UAV size and performance. Code can be improved by adding empirical data, more detailed aero and structural models which are specific to companies in the extent of their experience, tested products and matured technologies.

Table 3. Input parameters and values for Conf.1 (Chaput, 2004; Raymer, 1999; Honeywell, 2014; Defense Technical Information Center, 2003; Executive Aircraft Maintenance, 2014)

Mission Parameters	**Value**
h_0	0 [km]
h_{10}	0
h_{34}	6,096
h_{56}	9,144
h_{78}	9,144
h_9	6,096
R_{op}	472,3
t_{idle}	20
PLA_{idle}	10 %
t_{pow}	5
t_{wait}	20
$f_{resfuel}$	0,03
Weight Parameters	**Value**
W_{Pi}	363
W_{Pe}	454
W_{fi}	907
W_{fe}	862
f_{lg}	0,043
f_{sys}	0,12
f_{misc}	0,02
f_{wm}	0,03
u_{fus}	19
u_{wing}	32
u_{htail}	18
u_{vtail}	18
ρ_{fuel}	801
ρ_{eng}	449
ρ_{lg}	256
ρ_{sys}	256
ρ_{pl}	272
C_{ff}	0,9
C_{fw}	0,85
C_{fht}	0,83
C_{fvt}	0,83
Aerodynamic Parameters	**Value**
C_{fe}	0,0041
C_{Lmax}	1,8
$C_{L,\ TO}$	1,49
e	0,75
V_{wind}	0
V_{climb}/V_{stall}	1,25

V_{loiter}/V_{stall}	1,1
V_{cr}	370
V_{loi}	0,4
V_{ref}	185,2
Airframe Parameters	**Value**
n_{fus}	1
$L_{fus}/Ø_{fus}$	10,75
$L_{fus.b}/L_{fus}$	0,1
$f_{fus.vol}$	0,7
$f_{fus.vol.m}$	1,3
Wing Parameters	**Value**
AR	17,92
W/S	210,8
λ	0,444
t/c	0,13
t_{ave}/t_{max}	0,6
V_{fuel}/V_{wing}	0,5
Tail Parameters	**Value**
S_h/S	0,08
S_v/S	0,135
Nacelle Parameters	**Value**
$L_{nac}/Ø_{nac}$	2,7
$Ø_{nac}/Ø_{eng}$	1,25
$f_{nac.wet}$	0,5
L_{nac}/L_{fus}	0,5
Engine parameters	**Value**
n_{eng}	1
$f_{th.ins}$	0,9
$f_{w.eng}$	1,3
F_{net}/W_0	0,3359 [kgf/kg]
T_4	1368,7
Π_C	10,37
$\eta_{C,pol}$	0,795
$\eta_{T,pol}$	0,86
η_b	0,999
η_m	0,995
ΔP_{in}	0
ΔP_b	0,03
$\Delta P_{t.duct}$	0,025
$\Delta P_{i.pipe}$	0,02
N_{cd}	1
N_{cx}	0,99
Π_N	1,03
β_1	0
ε_1	0
ε_{2a}	0,05
ε_{2b}	0
ε_3	0,05
$Ø_{prop}$	2,8
Ω_{prop}	1591
$\eta_{prop,d}$	0,8
$\eta_{prop,s}$	0,7

Table 5. Turboprop engine cycle calculations comparison.

Engine Parameter	**Max difference from GasTurb**
PW	0,37%
EPW	0,10%
ESFC	0,51%
TSFC	0,85%
F_{net}	0,46%
P_i	0,11%
T_i	0,13%

Table 4. Result parameters and values.

Aircraft output parameters										
W_0	4770									
S	22,61									
R	9308									
t_{loi}	28,96									
t_{CR}	2,32									
t_{tot}	32,20									
E	31,28									
d_{cl}	85,20									
Mission points	#1	#2	#3	#4	#5	#6	#7	#8	#9	#10
h	0,000	0,000	6,096	6,096	9,144	9,144	9,144	9,144	6,096	0,000
M_0	0,151	0,182	0,268	0,326	0,339	0,329	0,270	0,339	0,326	0,145
C_L	1,274	0,878	0,870	0,590	0,825	0,878	0,878	0,556	0,381	0,878
V_0	185,2	222,6	304,9	370,4	370,4	359,0	294,7	370,4	370,4	177,8
L/D	22,46	24,03	24,03	22,24	23,99	24,03	24,03	21,73	17,55	24,03
W	4762	4743	4697	4697	4618	4618	3112	3112	3037	3037
D	2078	1935	1917	2070	1887	1884	1269	1404	1696	1235
Engine output parameters										
PW	712	719	462	476	356	354	343	356	476	711
EPW	739	752	485	504	375	372	358	375	504	737
$PSFC_{uninstalled}$	0,324	0,323	0,282	0,278	0,265	0,266	0,269	0,265	0,278	0,325
$ESFC_{uninstalled}$	0,312	0,309	0,269	0,263	0,252	0,253	0,258	0,252	0,263	0,313
T_{inst}	11310	9503	4425	3730	2787	2862	3399	2787	3730	11757
$TSFC_{uninstalled}$	5,673	6,782	8,184	9,864	9,408	9,133	7,562	9,408	9,864	5,453
$\mathbf{w}_i$	3,540	3,561	1,803	1,840	1,246	1,241	1,215	1,246	1,840	3,536
P_0	103,0	103,7	48,9	50,1	32,6	32,4	31,7	32,6	50,1	102,8
P_2	103,0	103,7	48,9	50,1	32,6	32,4	31,7	32,6	50,1	102,8
P3	1067,7	1075,2	507,6	519,7	337,9	336,3	328,3	337,9	519,7	1066,3
P_{31}	1067,7	1075,2	507,6	519,7	337,9	336,3	328,3	337,9	519,7	1066,3

P_4	1035,6	1043,0	492,4	504,1	327,8	326,2	318,4	327,8	504,1	1034,3
P_{41}	1035,6	1043,0	492,4	504,1	327,8	326,2	318,4	327,8	504,1	1034,3
P_{416}	261,4	262,5	151,3	153,5	110,6	110,2	108,5	110,6	153,5	261,3
P_{44}	261,4	262,5	151,3	153,5	110,6	110,2	108,5	110,6	153,5	261,3
P_{46}	256,2	257,2	148,2	150,4	108,4	108,0	106,3	108,4	150,4	256,0
P_{48}	104,9	104,9	48,2	48,2	31,1	31,1	31,1	31,1	48,2	104,9
P_5	104,4	104,4	48,0	48,0	31,0	31,0	31,0	31,0	48,0	104,4
T_0	289,5	290,1	252,1	253,8	234,0	233,7	232,1	234,0	253,8	289,4
T_2	289,5	290,1	252,1	253,8	234,0	233,7	232,1	234,0	253,8	289,4
T_3	660,0	661,3	579,3	583,0	539,4	538,7	535,1	539,4	583,0	659,8
T_{31}	660,0	661,3	579,3	583,0	539,4	538,7	535,1	539,4	583,0	659,8
T_4	1368,7	1368,7	1368,7	1368,7	1368,7	1368,7	1368,7	1368,7	1368,7	1368,7
T_{41}	1334,9	1335,0	1331,5	1331,7	1329,9	1329,9	1329,7	1329,9	1331,7	1334,9
T_{416}	1007,0	1006,3	1047,0	1045,1	1066,4	1066,7	1068,5	1066,4	1045,1	1007,1
T_{44}	990,9	990,4	1025,6	1024,1	1042,5	1042,8	1044,4	1042,5	1024,1	991,0
T_{46}	990,9	990,4	1025,6	1024,1	1042,5	1042,8	1044,4	1042,5	1024,1	991,0
T_{48}	818,5	817,3	807,4	803,5	800,0	800,8	804,8	800,0	803,5	818,7
T_5	818,5	817,3	807,4	803,5	800,0	800,8	804,8	800,0	803,5	818,7
T_7	818,5	817,3	807,4	803,5	800,0	800,8	804,8	800,0	803,5	818,7

Equations

For the sizing of UAV, general weight formulae:

$W_0 = W_e + W_{PL} + W_f + W_{misc}$ (1)
$W_e = W_{af} + W_{lg} + W_{eng} + W_{sys}$ (2)
$W_{af} = W_{fus} + W_{nac} + W_{h.tail} + W_{v.tail}$ (3)

Flight durations and range calculations:

$R_F = R_{CL} + R_{CR} + R_D$ (4)
$t_F = t_{CL} + t_{CR} + t_D$ (5)
$t_B = t_F + t_{GR}$ (6)
$R_{CR} = \frac{V_0}{C}\frac{L}{D}\ln\frac{W_{i-1}}{W_i}$ (7)

$t_{CR} = \frac{L/D}{C}\ln\frac{W_{i-1}}{W_i}$ (8)

A two spool turboprop engine design point calculation:

$$T_0 = T_{amb}\left[1+\left(\frac{\gamma-1}{2}\right)M^2\right] \quad (9)$$

$$P_0 = P_{amb}\left[1+\left(\frac{\gamma-1}{2}\right)M^2\right]^{\frac{\gamma}{\gamma-1}} \quad (10)$$

Intake:

$$T_2 = T_0 \quad (11)$$

$$P_2 = P_0 * (1-\Delta P_{in}) \quad (12)$$

$$C_{corr} = \frac{\delta\left[1+\left(\frac{\gamma-1}{2}\right)M^2\right]^{\frac{\gamma}{\gamma-1}}}{\left[\theta\left(1+\left(\frac{\gamma-1}{2}\right)M^2\right)\right]^{\frac{1}{2}}} \quad (13)$$

$$C_{corr} = \frac{P_0/P_{SL}}{[T_0/T_{SL}]^{\frac{1}{2}}} \quad (14)$$

Compressor section:

$$\eta_2 = \frac{(\Pi_C)^{\frac{\gamma_C-1}{\gamma_C}}-1}{(\Pi_C)^{\frac{\gamma_C-1}{\gamma_C*\eta_{C,pol}}}-1} \quad (15)$$

$$T_3 = T_2\left(1+\frac{1}{\eta_2}(\Pi_C{}^{\frac{\gamma-1}{\gamma}}-1)\right) \quad (16)$$

$$P_3 = P_2\Pi_C \quad (17)$$

Compressor exit airflow:

$$w_3 = w_2 - w_2(\beta_1+\varepsilon_1) \quad (18)$$

$$T_{bleed} = \frac{T_3+T_2}{2} \quad (19)$$

$$G_C = w_3 C_{PC}(T_3 - T_2) + (w_2 - w_3)C_{PC}(T_{bleed} - T_2) \quad (20)$$

Compressor exit diffuser:

Total temperature does not change, total pressure reduces by a ratio. Moreover, air mass flow rate is reduced due to bleed and cooling air extraction.

$$T_{31} = T_3 \quad (21)$$

$$P_{31} = P_3 \quad (22)$$

$$w_{31} = w_3 - w_2(\varepsilon_{2a}+\varepsilon_{2b}+\varepsilon_3) \quad (23)$$

Combustor and NGV station:

$$P_4 = P_{31}(1-\Delta P_b) \quad (24)$$

f, fuel air ratio calculation:

$f_1 = 0{,}10118 + (2{,}00376e\text{-}05)(700 - T_{31})$ (25)
$f_2 = 3{,}7078e\text{-}03 - (5{,}2368e\text{-}06)(700 - T_{31}) - (5{,}2632e\text{-}06)T_4$ (26)
$f_3 = (8{,}889e\text{-}08)\,\mathrm{abs}(T_4-950)$ (27)
$f = (f_1 - (f_1^2 + f_2)^{1/2} - f_3)/\eta_b$ (28)
$w_f = f(w_{31} + w_2\varepsilon_3)$ (29)
$w_4 = w_{31} + w_f$ (30)
$w_{41} = w_{31} + w_2\varepsilon_3 + w_f$ (31)
$T_{41} = \frac{(w_4 C_{PT} T_4 + w_2\varepsilon_3 C_{PC} T_{31})}{w_{41} C_{PT}}$ (32)
$P_{41} = P_4$ (33)

No total pressure loss is assumed at NGV.

High pressure turbine:

$G_{HPT} = G_C/\eta_m$ (34)
$T_{416} = T_{41} - G_{HPT}/(w_{41} C_{PT})$ (35)

HPT isentropic efficiency can be calculated by assuming Π_T (Turbine total pressure ratio) an initial value (such as 4):

$$\eta_{416} = \frac{1 - \Pi_T^{\frac{(1-\gamma_T)\eta_{T,pol}}{\gamma_T}}}{1 - \Pi_T^{\frac{1-\gamma_T}{\gamma_T}}} \quad (36)$$

$$\Pi_T = \frac{e^{\log\left(1 - \frac{T_{41} - T_{416}}{\eta_{416}\, T_{41}}\right)}}{\frac{1-\gamma_T}{\gamma_T}} \quad (37)$$

If equations (4.46) and (4.47) are iterated 3-5 times, Π_T and η_{416} values converge.

high pressure türbin total pressure:

$$P_{416} = P_4 / \Pi_T \quad (38)$$
$$w_{416} = w_{41} \quad (39)$$

Rotor cooling air addition is done numerically at Station 44 (Kurzke, 2007):

$$w_{44} = w_{416} + w_2 \varepsilon_{2a} \quad (40)$$

$$T_{44} = \frac{(w_{416} C_{PT} T_{416} + w_2 \varepsilon_{2a}\ C_{PC}\ T_{31})}{w_{44} C_{PT}} \quad (41)$$

$$P_{44} = P_{416} \quad (42)$$

Turbine duct (between HPT and LPT):

Total temperature does not change, but total pressure is reduced.

$$T_{46} = T_{44} \quad (43)$$
$$P_{46} = P_{416}(1 - \Delta P_{t.duct}) \quad (44)$$
$$w_{46} = w_{44} \quad (45)$$

Low pressure turbine:

$$P_5 = \Pi_N P_{amb} \quad (46)$$

Where Π_N, exhaust nozzle pressure ratio is a design input.

$$P_{48} = P_5 / (1 - \Delta P_{j.pipe}) \quad (47)$$
$$\Pi_T = P_{46} / P_{48} \quad (48)$$

$$\eta_{46} = \frac{1 - \Pi_T^{\frac{(1-\gamma_T)\eta_{T,pol}}{\gamma_T}}}{1 - \Pi_T^{\frac{1-\gamma_T}{\gamma_T}}} \quad (49)$$

$$T_{48} = T_{46}\left(1 - \eta_{46}\left(1 - \Pi_T^{\frac{1-\gamma_T}{\gamma_T}}\right)\right) \quad (50)$$
$$G_{LPT} = (T_{46} - T_{48})(w_{46} C_{PT}) \quad (51)$$
$$PW = G_{LPT}\, \eta_m \quad (52)$$

Low pressure turbine exit:

$$w_{48} = w_{46} \quad (53)$$
$$w_5 = w_{48} + w_2 \varepsilon_1 + w_2 \varepsilon_{2b} \quad (54)$$

$$T_5 = \frac{w_{48} C_{PT} T_{48} + w_2 \varepsilon_1 C_{PC} T_{bleed} + w_2 \varepsilon_{2b} C_{PC} T_{31}}{w_5 C_{PT}} \quad (55)$$

Exhaust Nozzle:

$$T_7 = T_5 \quad (56)$$
$$w_7 = w_5 \quad (57)$$

Nozzle pressure ratio in choked condition:

$$P_5/P_{7s,c} = \left[\frac{1+\gamma_C}{2}\right]^{\left(\frac{\gamma_C}{\gamma_C - 1}\right)} \quad (58)$$

If, design nozzle pressure ratio $\Pi_N > P_5/P_{7s,c}$ than the nozzle is choked and M_7 is equal to 1. Choked nozzle exit static temperature:

$$T_{7s,c} = \left[\frac{T_5}{1 + \frac{\gamma_T - 1}{2}}\right] \quad (59)$$

$$a_7 = \left[\gamma_T R T_{7s,c}\right]^{\frac{1}{2}} \quad (60)$$

$$A7,c = \frac{0.001 w_5}{N_{cd} \frac{P_5}{(T_5)^{1/2}} \left(\frac{\gamma_T}{R}\right)^{1/2} \left(\frac{(\gamma_T + 1)}{2}\right)^{\frac{-\gamma_T - 1}{2(\gamma_T - 1)}}} \quad (61)$$

$$F_A = w_5\, a_7 + A_{7,c}\, N_{cd}\, (P_{7s,c} - P_{amb})\, 1000 \quad (62)$$

If nozzle is not choked, M_7 is not 1 and can be calculated as follows:

$$M_7 = \left[\frac{2}{\gamma_T - 1}\left[\left(\frac{P_{amb}}{P_5}\right)^{\frac{1-\gamma_T}{\gamma_T}} - 1\right]\right]^{\frac{1}{2}} \quad (63)$$

$$T_{7s} = \left[\frac{T_5}{1 + \frac{\gamma_T - 1}{2} M_7^2}\right] \quad (64)$$

$$a_7 = \left[\gamma_T R T_{7s}\right]^{\frac{1}{2}} \quad (65)$$
$$F_A = w_7\, a_7\, M_7 \quad (66)$$

Propeller Thrust Calculation:

$$J = \frac{V_0}{n} d \quad (67)$$

$$C_{PW} = \frac{PW}{n^3 d^5 \rho} \quad (68)$$

$$C_F = \frac{\eta_{prop,d} C_{PW}}{J} \quad (69)$$

for static conditions (V_0=0) :

$$C_F = (\eta_{prop,s} C_{PW})^{2/3} (\pi / 2)^{1/3} \quad (70)$$

$$F_P = \frac{C_F PW}{C_{PW} nd} \quad (71)$$

Total Thrust and SFC:

$$V_0 = M_0 (\gamma_C R T_{amb})^{1/2} \quad (72)$$
$$F_{net} = F_P + F_A N_{cx} - w_2 V_0 \quad (73)$$
$$TSFC = w_f / F_{net} \quad (74)$$
$$PSFC = w_f / PW \quad (75)$$
$$EPW = PW + V_0 F_A / \eta_p \quad (76)$$
$$ESFC = w_f / EPW \quad (77)$$

REFERENCES

Austin R., 2010, Unmanned Aircraft Systems, Wiley, West Sussex, UK.

Buğdaycı H., 1980, Study of Effects of Performance of Aircraft to the Aircraft Operation Characteristics, Ph.D. Thesis, İstanbul Technical University, İstanbul.

Chaput J.A., 2004, Conceptual Design of UAV Systems, Lecture Notes, University of Texas, Austin, TX.

Chaput J.A., 2010, Rapid Air System Concept Exploration – A Parametric Physics Based System Engineering Design Model, AIAA Aviation Technology, Integration, and Operations Conference, Fort Worth, TX.

Curtis H., Filippone A., Cook M., Jenkinson, L.R. and De Florio F., 2009, Aerospace Engineering Desk Reference (First Ed.), Butterworth-Heinemann, San Diego, CA, 7.

Defense Technical Information Center, 2003, Predator B: The Multi-Role UAV, http://www.dtic.mil/get-tr-doc/pdf?AD=ada427459

Department of Defense, 2009, FY2009–2034 Unmanned Systems Integrated Roadmap, USA.

Department of the Air Force Headquarters Air Force Civil Engineer Support Agency, 2009, Airfield Planning and Design Criteria for Unmanned Aircraft Systems, http://www.wbdg.org/ccb/AF/AFETL/etl_09_1.pdf

Executive Aircraft Maintenance, 2014, TPE331 Turboprop Evolution, http://www.eamaz.com/uploads/Master_-_TPE331_Turboprop_Evolution.pdf

Federation of American Scientists, 2014, Air Combat Command Concept of Operations for Endurance Unmanned Aerial Vehicles, http://www.fas.org/irp/doddir/usaf/conops_uav/part03.htm

Genç M.S., Özişik G. and Kahraman N., 2008, Investigation of Aerodynamics Performance of NACA0012 Aerofoil with Plain Flap, J. of Thermal Science and Technology, 28, 1, 1-8.

General Atomics Aeronautical Systems, 2014, Product Brochures, http://www.ga-asi.com/products/aircraft/pdf/Predator_B.pdf

Honeywell, 2014, Product Brochures, http://www51.honeywell.com/aero/common/documents/myaerospacecatalog-documents/BA_brochures-documents/TPE331-10_PredatorB_0292-000.pdf

Internet, 2014, ADS - Aircraft Design Software http://www.pca2000.com/en/index.php

İlbaş M. and Türkmen M., 2012, Estimation of Exhaust Gas Temperature Using Artificial Neural Network in Turbofan Engines, J. of Thermal Science and Technology, 32, 2, 11-18.

Kurzke J., 2007, Design and Off-Design Performance of Gas Turbines, GasTurb 11 User Manual, J. Kurzke, Munich, Germany.

Mattingly J., Heiser W. and Pratt D., 2002, Aircraft Engine Design (Second Ed.), AIAA Series, Washington, DC, 95.

Nicolai L.M., Carichner G., 2010, Fundamentals of Aircraft and Airship Design, AIAA Series, Washington, DC.

Raymer D.P., 1999, Aircraft Design: A Conceptual Approach (Third Ed.), AIAA Series, Washington, DC.

Roskam, J., 1990, Airplane Design, Parts I - VIII, DAR Corporation

Şahin Z., Kopaç M. and Aydin N.Ö., 2011, The Investigation of Increasing of the Efficiency in the Power Plant with Gas-Solid Fuels by Exergy Analysis, J. of Thermal Science and Technology, 31, 1, 85-107.

Turan Ö., Orhan İ. and Karakoç T.H., 2008, On-Design Analysis of High Bypass Turbofan Engines, Journal of Aeronautics and Space Technologies, 3, 3, 1-8.

UK Royal Air Force, 2014, Royal Air Force Reaper MALE RPAS Capability/Lessons, http://dronewarsuk.files.wordpress.com/2011/10/rpas_symposium_reaper.pdf

Uzol O., 2011, A New High-Fidelity Transient Aerothermal Model for Real-Time Simulations of the T700 Helicopter Turboshaft Engine, J. of Thermal Science and Technology, 31, 1, 37-44.

Walsh P. P., and Fletcher P., 2004, Gas Turbine Performance (Second Ed.), Blackwell, Oxford, UK.

DISCLAIMER

The views and opinions expressed in this article are those of the author and do not represent the official policy or position of Tusaş Engine Industries Inc. or any other company and institution.

Ali DİNÇ

Ali DİNÇ was born in 1970. He graduated from the department of Aeronautical Engineering, Middle East Technical University (METU) in 1992. He earned his MSc degree in 1995 within the scope of a cooperation project between METU and Tusaş Engine Ind. Inc. (TEI). Then, he worked for TEI in different positions of design engineering and management levels in aircraft engine components design area. In this context, he has worked for TEI in the design offices of General Electric-USA and ITP-Spain for a total of 5 years for the development of T38/J85 engine exhaust module design and A400M/TP400 turboprop engine development projects, respectively. He received his PhD degree at Anadolu University, School of Civil Aviation in 2010. He currently works as a senior engineer in Chief Engineering Office of TEI.